第 30 卷第 7 期
2013 年 7 月

控 制 理 论 与 应 用
Control Theory & Applications

Vol. 30 No. 7
Jul. 2013

DOI: 10.7641/CTA.2013.12213

双闭环策略下非完整轮式机器人鲁棒自适应运动/力协调控制

岳 明[1,2†], 王 爽[1], 张永顺[3]

(1. 大连理工大学 汽车工程学院, 辽宁 大连 116024;

2. 机械传动国家重点实验室 重庆大学, 重庆 400044; 3. 大连理工大学 机械工程学院, 辽宁 大连 116024)

摘要: 非完整轮式移动机器人的路径跟踪, 需要在保证机器人姿态跟踪精度的同时, 增强其地面适应性能. 为实现这种运动/力的协调控制目标, 本文提出双闭环的控制系统结构: 外环能够增加运动精度, 内环则可以增强机器人对地面动态摩阻的适应性. 同时, 考虑到地面摩阻的慢时变性, 本文通过构造观测器对其进行估计. 在具体算法实现方面, 采用反步法在外环构建运动控制器: 而在内环, 则是应用积分型的滑模技术设计力控制器与观测器. 最后, 对控制系统进行仿真, 仿真结果证明所提出控制方法的有效性.

关键词: 轮式机器人; 运动/力; 协调控制; 双闭环

中图分类号: TP242 **文献标识码**: A

Adaptive robust motion/force coordinated control of nonholonomic wheeled mobile robot via a double closed-loop strategy

YUE Ming[1,2†], WANG Shuang[1], ZHANG Yong-shun[3]

(1. School of Automotive Engineering, Dalian University of Technology, Dalian Liaoning 116024, China;

2. State Key Laboratory of Mechanical Transmission, Chongqing University, Chongqing 400044, China;

3. School of Mechanical Engineering, Dalian University of Technology, Dalian Liaoning 116024, China)

Abstract: Path following of a nonholonomic wheeled mobile robot should harmoniously guarantee the accurate robot posture tracking and the enhancing terrain-adaptive performance. To realize this coordinated motion/force objective, we propose a double closed-loop control structure with the outer loop to improve the motion accuracy and the inner loop to enhance the dynamic terrain friction adaptability. Meanwhile, the uncertain terrain friction is estimated by an observer considering its slow time-varying characteristic. In order to realize the control algorithms, we developed the motion controller for the outer loop via backstepping method; and apply the integral sliding mode technique to design the observer and the force controller for the inner loop. Simulations are performed and the results demonstrate the effectiveness of the proposed control schemes.

Key words: wheeled mobile robot; motion/force; coordinated control; double closed-loop

1 Introduction

Wheeled mobile robot is attracted a great deal of attentions in recent years due to the nature of nonholonomic constraints. Many efforts are devoted to the tracking control of nonholonomic mobile robots[1–3]. The nonholonomic constraint is introduced on system kinematic level which is only related to the robot's posture and velocities. Because of the nonintegrable characteristic of nonholonomic system, more state variables should be controlled by less control inputs, and so the nonholonomic system is substantively an underactuated system[4–5].

Moreover, most of control schemes ignore the dynamic disturbances such as the unavoidable terrain friction acting on the wheels. It is well-known that the dynamic disturbances is an important part for the design of controlling system, especially for a practical mobile robot in the real environment. However, different from the nonholonomic issue, this terrain friction is in the force form that is related to the system dynamic level. Therefore, how to both guarantee the posture tracking precision under nonholonomic constraint and enhance the disturbance adaptivity is a challenging problem to be resolved.

This problem is a motion/force coordinated control issue, where the system on kinematic level and dynamic level should be considered simultaneously. Lots of investigations address posture tracking control[6–7], and most studies report dynamic control of mobile robot[8–9]; however, only a few of literatures discuss the harmonious motion/force control problems. Li had investigated an adaptive robust motion/force control for wheeled inverted pendulums with parametric and functional uncertainties[10–11]. Hashemi had addressed a PI-fuzzy controller to realize

Received 13 September 2012; revised 22 March 2013.
†Corresponding author. E-mail: yueming@dlut.edu.cn; Tel.: +86 15941107498.
This research was supported by the National Natural Science Foundation of China (Nos. 61175101, 61175102), the State Key Laboratory of Mechanical Transmission (No. SKLMT-KFKT-201006) and the Fundamental Research Funds for the Central Universities (No. DUT12LK45).

path following and meanwhile, the anti-slippage objective had also been achieved in [12]. Yue had proposed a sliding mode robust control method for a two wheeled mobile robot with lower center of gravity, where the posture tracking and dynamic characteristic of mass center were both considered together [2, 13]. Motivated by these works, we propose a double closed-loop control structure and improve it with an observer scheme to estimate the uncertain disturbance in this study. This improved double closed-loop control strategy is essentially a two feedbacks structure and could realize the motion/force coordinated control. Particularly, since the desired trajectories are generated online under the double closed-loop control structure, it ought to assure that the convergence rate of the outer loop should be slower than that of the inner one. Such treatment could guarantee the global control performances of both inner and outer loops.

Furthermore, the backstepping technique is widely used as one of the representative methods for controlling nonholonomic mobile robot [14–16]. Then, we adopt this method to construct the motion controller on system's outer loop. Here, a simple function $x/(1+x^2)$ is applied to connect a relationship between two related state variables. Additionally, the sliding mode control technique is also employed to derive the control algorithms due to their better robustness and parameter insensibility [17]. Meanwhile, an integral sliding mode surface and continuously differentiable hyperbolic tangent function are adopted in this study to suppress the inherent chattering behaviors of the sliding mode method [18–19].

The organization of this paper is as follows: some preliminaries about nonholonomic wheeled mobile robot including mathematic model and double closed-loop control structure are described in Section 2. Section 3 reports the motion controller to realize the robot's postures tracking. While in Section 4, the force controller besides the observer scheme is addressed. Simulation study is developed in Section 5, and finally, some conclusions are summarized.

2 Preliminaries

2.1 A nonholonomic wheeled mobile robot

A typical mobile robot considered in this case has two actuators and a steering wheel, as illustrated in Fig.1. Here, r and R represent the wheel radius and the half width of the robot, respectively. For simplify, it is supposed that the mass center is coincident with the robot's centroid, i.e., the mass center $C(x_c,\ y_c)$ locates on the axis center between the two wheels. Then, the robot's postures could be described by three system state variables: the two coordinates of the gravity center $(x_c,\ y_c)$ and the orientation angle θ of the robot. Therefore, a general dynamic model of wheeled robot can be governed by

$$M(q)\ddot{q}+V_m(q,\dot{q})\dot{q}+F(\dot{q})+G(q)= \\ B(q)\tau-A^T(q)\lambda, \tag{1}$$

where $q=[x_c\ \ y_c\ \ \theta]^T\in\mathbb{R}^3$, $\tau\in\mathbb{R}^2$ represent state, input vectors of the system, respectively. $M(q)$ is a symmetric positive definite inertia matrix; $V_m(q,\dot{q})$ is a centripetal and coriolis matrix and it should be noted that $V_m(q,\dot{q})=0$ if the mass center is coincident with the centroid; $F(\dot{q})$ and $G(q)$ denote the surface friction and gravity matrix, and in this case they are supposed to zero since the robot operates on the plane; $B(q)$ represents input transformation matrix; λ and $A(q)$ are all related to the system nonholonomic constraints. The elements of the matrices in system (1) can be achieved in [2] for more details.

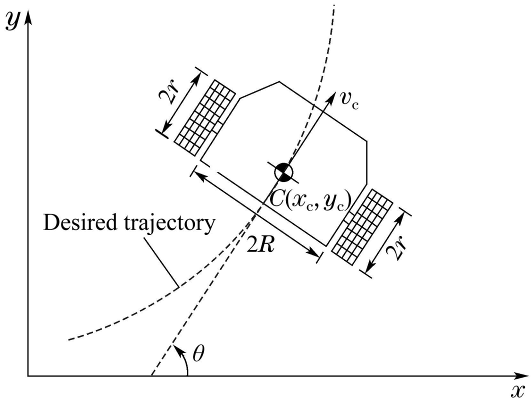

Fig. 1 The nonholonomic wheeled mobile robot

Meanwhile, the nonholonomic constraint of pure rolling and non-slipping can be described as

$$\begin{bmatrix}\dot{x}_c\\ \dot{y}_c\\ \dot{\theta}\end{bmatrix}=\begin{bmatrix}\cos\theta & 0\\ \sin\theta & 0\\ 0 & 1\end{bmatrix}\begin{bmatrix}v_c(t)\\ \omega_c(t)\end{bmatrix}=S(q)\nu_c(t), \tag{2}$$

where $S(q)\in\mathbb{R}^{3\times2}$ and $\nu_c(t)=[v_c(t)\ \ \omega_c(t)]^T\in\mathbb{R}^2$ are the velocity transformation matrix and velocity vector, respectively. Here, $v_c(t)\in\mathbb{R}$ denotes the linear velocity of the mass center and $\omega_c(t)\in\mathbb{R}$ indicts the angular velocity of the mobile robot. Obviously, this is a typical nonholonomic constraint because it could not be integrated to be a linear relationship between the system state variables. This nonholonomic system (2) is also defined as steering system of wheeled mobile robot.

Note that $S(q)$ is the null space of the matrix, i.e., $S^T(q)A^T(q)=0$. Differentiating (2) and substituting the result in (1), and then multiplying by $S^T(q)$, the constraint matrix $A^T(q)$ can be eliminated with this condition. Then, another dynamic form of wheeled mobile robot is achieved by

$$(S^TB)^{-1}S^TMS\dot{\nu}_c+ \\ (S^TB)^{-1}S^T(M\dot{S}+V_mS)\nu_c+\tau_d=\tau, \tag{3}$$

where $\tau_d=[\tau_{dl}\ \tau_{dr}]^T$ is introduced to represent disturbances for the terrain friction on robot's wheels with the form of force. For simplify, the system (3) can be rewritten as follows:

$$\bar{M}(q)\dot{\nu}_c+\bar{V}_m(q,\dot{q})\nu_c+\tau_d=\tau, \tag{4}$$

where $\bar{M}(q)=(S^TB)^{-1}S^TMS\in\mathbb{R}^{2\times2}$ is a symmetric positive definite inertia matrix, $\bar{V}_m(q,\dot{q})=(S^TB)^{-1}\times S^T(M\dot{S}+V_mS)\in\mathbb{R}^{2\times2}$ is the centripetal and coriolis matrix. System (4) describes the behavior of the nonholonomic system in a new set of local coordinates. Therefore, the properties of the original dynamics hold for this new set of coordinates.

2.2 Double closed-loop control structure

To realize the coordinated control of both motion and force behaviors of the mobile robot, a double closed-loop control structure is proposed, as shown in Fig.2. Such control strategy is essentially a two feedback structure. On outer loop, the steering system which is related to robot's postures could be controlled by motion controller. The nonholonomic constraint affected on the steering system is a challenging issue on the outer loop. Here, we adopt backstepping technique to resolve this problem by which could enhance tracking precision of the robot's postures. While, on inner loop, the dynamic model of mobile robot is controlled by a force controller. The disturbance in force form acting on the robot's wheels is unavoidable which should be considered in force controller. To solve this problem, an disturbance adaptive scheme is introduced and it can estimate the dynamic disturbance value on line. In addition, the sliding mode technique is applied to derive the dynamic controller by which could increase the adaptivity and robustness of the robot system.

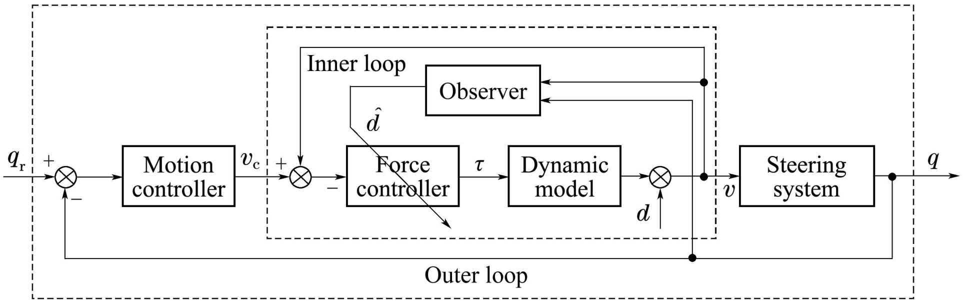

Fig. 2 Double closed-loop control structure

It should be noted that the outer and inner loops are strongly interrelated and reacted upon each other. The virtual velocity vector produced by the motion controller of outer loop is just the desired trajectory of inner loop. Therefore, this virtual velocity vector is building up the relationship between the system's kinematic and dynamic subsystem directly. Besides, it should also be noted that the driving torque produced on inner loop by force controller is the practical system input to the mobile robot because the velocity vector is indeed a virtual intermediate variables.

If the desired reference trajectory of the postures of robot are described by $q_r(t) = [x_r(t)\ \ y_r(t)\ \theta_r(t)]^T$, the current postures are $q = [x_c(t)\ \ y_c(t)\ \ \theta(t)]^T$ and the practical and virtual velocity vector is represented by $\nu,\ \nu_c$, respectively, the whole control objectives of the mobile robot might be summarized up as follows:

Step 1 Find an appropriate control input $\nu_c = [\upsilon_c(t)\ \ \omega_c(t)]^T$ such that $\lim\limits_{t\to\infty} q(t) = q_r(t)$;

Step 2 Find an appropriate control input $\tau = [\tau_l\ \ \tau_r]^T$ such that $\lim\limits_{t\to\infty} \nu(t) = \nu_c(t)$;

Step 3 Find a coordinated control input $\tau = [\tau_l\ \ \tau_r]^T$ such that $\lim\limits_{t\to\infty} q(t) = q_r(t)$.

3 Motion controller

On outer loop, to achieve the tracking performance of $q \to q_r$ as $t \to \infty$, a tracking error space

$$q_e = [x_e\ \ y_e\ \ \theta_e]^T$$

should be introduced as follows[20]:

$$q_e = \begin{bmatrix} x_e \\ y_e \\ \theta_e \end{bmatrix} = \begin{bmatrix} \cos\theta & \sin\theta & 0 \\ -\sin\theta & \cos\theta & 0 \\ 0 & 0 & 1 \end{bmatrix} \begin{bmatrix} x_r - x_c \\ y_r - y_c \\ \theta_r - \theta \end{bmatrix}.$$

Obviously, $(x_e, y_e, \theta_e) = 0$ if and only if $(x_c, y_c, \theta) = (x_r, y_r, \theta_r)$ for any value of θ. Differentiating the above tracking errors and substituted $\dot{q}$ by (2), it can be obtained that:

$$\dot{q}_e = \begin{bmatrix} \dot{x}_e \\ \dot{y}_e \\ \dot{\theta}_e \end{bmatrix} = \begin{bmatrix} \upsilon_r \cos\theta_e + \omega_c y_e - \upsilon_c \\ \upsilon_r \sin\theta_e - \omega_c x_e \\ \omega_r - \omega_c \end{bmatrix}, \tag{5}$$

where $\upsilon_r,\ \omega_r \in \mathbb{R}$ are the desired linear and angular velocities of the mobile robot system respectively. Under system state error space, the tracking problem is transformed to find an appropriated control input $\nu_c = [\upsilon_c\ \omega_c]^T$, such that $\lim\limits_{t\to\infty} (|x_e(t)| + |y_e(t)| + |\theta_e(t)|) = 0$.

As can be seen in the tracking error model (5), the variable $\dot{y}_e = -x_e\omega_c + \upsilon_r \sin\theta_e$ is also controlled by the control input ω_c. It can be further concluded that $\dot{y}_e = -x_e\omega_c$ as $\theta_e = 0$. Suppose a Lyapunov function $V_y = y_e^2/2$, and an appropriated function, to which x_e should approach, ought to be find for driving $\dot{V}_y = y_e\dot{y}_e \leqslant 0$. Fortunately, we find that $\omega_c/(1+\omega_c^2)$ is such a function. Based on this consideration, the preliminary of the backstepping method is constructed. To sum up, if the appropriated υ and ω could be found to realize $x_e \to k_1 2\delta\omega_c/(1+\omega_c^2 y_e)$ and $\theta_e \to 0$, the stability of system (5) will be achieved. Then, we define a new variable $\bar{x}_e$ as follows:

$$\bar{x}_e = x_e - k_1 \frac{2\delta\omega_c}{1+\omega_c^2} y_e, \tag{6}$$

where k_1 and δ are all positive constants.

And then the differentiating $\bar{x}_e$ yields

$$\dot{\bar{x}}_e = \dot{x}_e - k_1 \frac{2\delta - 2\delta\omega_c^2}{\omega_c^4 + 2\omega_c^2 + 1} \dot{\omega}_c y_e - k_1 \frac{2\delta\omega_c}{1+\omega_c^2} \dot{y}_e. \tag{7}$$

According to system (5), when $x_e \to k_1 2\delta\omega_c y_e / (1+\omega_c^2)$ and $\theta_e \to 0$, it obtains that

$$\dot{y}_e = -x_e\omega_c = -k_1 \frac{2\delta\omega_c^2}{1+\omega_c^2} y_e. \tag{8}$$

Note that $\dot{V}_y = -k_1 2\delta\omega_c^2 y_e^2/(1+\omega_c^2)$, and obviously, $\dot{V}_y \leqslant 0$, i.e., the system will be stabilized. According to the proposed preliminary, a theorem can be achieved as follows:

Theorem 1 For $\forall t \in (0, +\infty)$, the system (5) will be globally stabilized, and the tracking error $\lim\limits_{t\to\infty}[|x_\mathrm{e}(t)| + |y_\mathrm{e}(t)| + |\theta_\mathrm{e}(t)|] = 0$, with the controllers as follows:

$$\omega_\mathrm{c} = \omega_\mathrm{r} + 2\upsilon_r k_3 y_\mathrm{e}\cos\frac{\theta_\mathrm{e}}{2} + k_4\sin\frac{\theta_\mathrm{e}}{2}, \tag{9}$$

$$\begin{aligned}\upsilon_\mathrm{c} = {}&\upsilon_\mathrm{r}\cos\theta_\mathrm{e} + k_1\frac{2\delta\omega_\mathrm{c}^2}{1+\omega_\mathrm{c}^2}x_\mathrm{e} - \\ &k_1\upsilon_\mathrm{r}\frac{2\delta\omega_\mathrm{c}}{1+\omega_\mathrm{c}^2}\sin\theta_\mathrm{e} - k_1\frac{2\delta - 2\delta\omega_\mathrm{c}^2}{\omega_\mathrm{c}^4 + 2\omega_\mathrm{c}^2 + 1}\dot{\omega}_\mathrm{c}y_\mathrm{e} + \\ &k_2x_\mathrm{e} - k_1k_2\frac{2\delta\omega_\mathrm{c}}{1+\omega_\mathrm{c}^2}y_\mathrm{e},\end{aligned} \tag{10}$$

where $k_1,\ k_2,\ k_3,\ k_4$ are all positive constants whose value could determine the control performances directly, and the $\dot{\omega}$ used in (10) can be achieved by

$$\begin{aligned}\dot{\omega}_\mathrm{c} = {}&\dot{\omega}_\mathrm{r} + 2k_3y_\mathrm{e}\dot{\upsilon}_\mathrm{r}\cos\frac{\theta_\mathrm{e}}{2} + \\ &2k_3(\upsilon_\mathrm{r}\sin\theta_\mathrm{e} - \omega_c x_\mathrm{e})\upsilon_\mathrm{r}\cos\frac{\theta_\mathrm{e}}{2} - \\ &k_3y_\mathrm{e}\upsilon_\mathrm{r}(\omega_\mathrm{r} - \omega_\mathrm{c})\sin\frac{\theta_\mathrm{e}}{2} + \frac{1}{2}k_4(\omega_\mathrm{r} - \omega_\mathrm{c})\cos\frac{\theta_\mathrm{e}}{2}.\end{aligned}$$

Proof Consider a candidate Lyapunov function as follows:

$$V_1(x_\mathrm{e}, y_\mathrm{e}.\theta_\mathrm{e}) = \frac{1}{2}\bar{x}_\mathrm{e}^2 + \frac{1}{2}y_\mathrm{e}^2 + \frac{2}{k_3}(1 - \cos\frac{\theta_\mathrm{e}}{2}).$$

As can be directly verified that V_1 is a positive-definite and radially unbounded function. Taking the time derivation of V_1 along trajectory of (5)–(7) yields

$$\begin{aligned}\dot{V}_1 = {}&\bar{x}_\mathrm{e}\dot{\bar{x}}_\mathrm{e} + y_\mathrm{e}\dot{y}_\mathrm{e} + \frac{1}{k_3}\sin\frac{\theta_\mathrm{e}}{2}\dot{\theta}_\mathrm{e} = \\ &\bar{x}_\mathrm{e}(\dot{x}_\mathrm{e} - k_1\frac{2\delta - 2\delta\omega_\mathrm{c}^2}{\omega_\mathrm{c}^4 + 2\omega_\mathrm{c}^2 + 1}\dot{\omega}_\mathrm{c}y_\mathrm{e} - k_1\frac{2\delta\omega_\mathrm{c}}{1+\omega_\mathrm{c}^2}\dot{y}_\mathrm{e}) + \\ &y_\mathrm{e}(\upsilon_\mathrm{r}\sin\theta_\mathrm{e} - x_\mathrm{e}\omega_\mathrm{c}) + \frac{1}{k_3}\sin\frac{\theta_\mathrm{e}}{2}(\omega_\mathrm{r} - \omega_\mathrm{c}) = \\ &\bar{x}_\mathrm{e}[(\upsilon_\mathrm{r}\cos\theta_\mathrm{e} - \upsilon_\mathrm{c} + y_\mathrm{e}\omega_\mathrm{c}) - \\ &k_1\frac{2\delta - 2\delta\omega_\mathrm{c}^2}{\omega_\mathrm{c}^4 + 2\omega_\mathrm{c}^2 + 1}\dot{\omega}_\mathrm{c}y_\mathrm{e} - \\ &k_1\frac{2\delta\omega_\mathrm{c}}{1+\omega_\mathrm{c}^2}(\upsilon_\mathrm{r}\sin\theta_\mathrm{e} - x_\mathrm{e}\omega_\mathrm{c})] + \\ &y_\mathrm{e}[-\omega_\mathrm{c}(\bar{x}_\mathrm{e} + k_1\frac{2\delta\omega_\mathrm{c}}{1+\omega_\mathrm{c}^2}y_\mathrm{e}) + \upsilon_\mathrm{r}\sin\theta_\mathrm{e}] + \\ &\frac{1}{k_3}\sin\frac{\theta_\mathrm{e}}{2}(\omega_\mathrm{r} - \omega_\mathrm{c}) = \\ &\bar{x}_\mathrm{e}[(\upsilon_\mathrm{r}\cos\theta_\mathrm{e} - \upsilon_\mathrm{c}) - k_1\frac{2\delta - 2\delta\omega_\mathrm{c}^2}{\omega_\mathrm{c}^4 + 2\omega_\mathrm{c}^2 + 1}\dot{\omega}_\mathrm{c}y_\mathrm{e} - \\ &k_1\frac{2\delta\omega_\mathrm{c}}{1+\omega_\mathrm{c}^2}(\upsilon_\mathrm{r}\sin\theta_\mathrm{e} - x_\mathrm{e}\omega_\mathrm{c})] - k_1\frac{2\delta\omega_\mathrm{c}^2}{1+\omega_\mathrm{c}^2}y_\mathrm{e}^2 + \\ &\frac{1}{k_3}\sin\frac{\theta_\mathrm{e}}{2}[(\omega_\mathrm{r} - \omega_\mathrm{c}) + 2k_3y_\mathrm{e}\upsilon_\mathrm{r}\cos\frac{\theta_\mathrm{e}}{2}].\end{aligned}$$

Substituting (9) and (10) into $\dot{V}_1$ indicates

$$\dot{V}_1 = -k_2\bar{x}_\mathrm{e}^2 - k_1y_\mathrm{e}^2\frac{2\delta\omega_\mathrm{c}^2}{1+\omega_\mathrm{c}^2} - \frac{k_4}{k_3}\sin^2\frac{\theta_\mathrm{e}}{2}.$$

Obviously, $\dot{V}_1 \leqslant 0$ for $\forall t \in (0, +\infty)$. By Lyapunov stability criterion, it can be concluded that for all initial conditions $q_\mathrm{e}(0)$, the corresponding solution $q_\mathrm{e}(t)$ converges to zero, i.e.

$$\lim_{t\to\infty}[|x_\mathrm{e}(t)| + |y_\mathrm{e}(t)| + |\theta_\mathrm{e}(t)|] = 0.$$

This proof is completed.

4 Force controller

4.1 Integral sliding mode technique

Different from the outer loop, the inner one should track the virtual velocity vector generated by the outer loop on line. Generally, the terrain friction acting on the wheels is in the form of torque, which can be considered as disturbance. Then we develop the dynamic model and explore force controller to enhance the robot's dynamic adaptability to this uncertain disturbance. If $\nu_\mathrm{c} = [\upsilon_\mathrm{c}\ \ \omega_\mathrm{c}]^\mathrm{T}$, $\nu = [\upsilon\ \omega]^\mathrm{T}$ represent the virtual velocity produced by motion controller and the current velocity measured by sensors, an auxiliary velocity tracking error vector could be introduced as $e_\nu = \nu_\mathrm{c} - \nu$. With this tracking error space, the tracking problem is thus transformed into a stabilization problem.

In order to guarantee the tracking performances of mobile robot, integral sliding mode control technique is applied to derive the system dynamic controller in this case, since integral sliding manifold has many better properties than the traditional sliding mode surface, such as robustness against the input channel parametric variations, and external disturbance rejection[21]. The integral sliding mode surface is constructed as follows:

$$\Im(t) = e_\nu + c\int_0^t e_\nu\mathrm{d}s, \tag{11}$$

where $c = [c_1\ c_2]$ is a positive matrix and $c_1,\ c_2 > 0$.

Suppose that the disturbance $\tau_\mathrm{d} = [\tau_\mathrm{dl}\ \tau_\mathrm{dr}]^\mathrm{T}$ in (4) is known well, its value can be directly used in the force controller. Then, the system control input can be given by:

$$\begin{aligned}\tau = {}&\bar{M}\dot{\nu}_\mathrm{c} + c\bar{M}e_\nu + \bar{V}_\mathrm{m}\nu_\mathrm{c} + \tau_\mathrm{d} + \\ &\bar{M}[\sigma_1\tanh(\kappa\Im) + \sigma_2\Im],\end{aligned} \tag{12}$$

where $\sigma_1,\ \sigma_2 > 0$ and $\kappa > 0$. Note that the hyperbolic tangent function $\tanh(\kappa\Im)$, by which the better chattering suppression characteristic could be achieved, is used in force controller to replace the signal function. The constant κ might determine the transient time.

To sum up, a theorem can be addressed as follows:

Theorem 2 The velocity tracking error $e_\nu = \nu_\mathrm{c} - \nu$ will asymptotically converge to zero, if the controller (12) is applied to system (4).

Proof A Lyapunov function candidate can be defined as

$$V_2 = \frac{1}{2}\Im^\mathrm{T}\Im.$$

Clearly, $V_2 > 0$. Differentiating V_2 yields

$$\begin{aligned}&\dot{V}_2 = \Im^\mathrm{T}\dot{\Im} = \\ &\Im^\mathrm{T}(ce_\nu + \dot{\nu}_\mathrm{c} - \bar{M}^{-1}\tau + \bar{M}^{-1}\bar{V}_\mathrm{m}\nu_\mathrm{c} + \bar{M}^{-1}\tau_\mathrm{d}).\end{aligned} \tag{13}$$

Substituting (12) into (13) achieves that

$$\dot{V}_2 = -\sigma_1\Im^\mathrm{T}\tanh(\kappa\Im) - \sigma_2\Im^\mathrm{T}\Im.$$

Obviously, $\dot{V}_2 \leqslant 0$. By Lyapunov stability theorem, the tracking errors converge to zero globally, and then the Theorem is proved.

4.2 Observer scheme

In practical application, the controller (12) based on the accurate disturbance value is unrealistic to be applied since the disturbance $\tau_{\rm d}$ is usually uncertain and could not be predicted in advance. Although the sliding mode control scheme might realize the system stabilization ultimately, however, this uncertain disturbance is mostly so great that it could result in violent chattering to the system variables around the sliding mode surface. Fortunately, it should be noted that, although the disturbances (terrain friction) are uncertain, the change rate of disturbances are much slower in practical exploration. Considering this fact, we determine to introduce an adaptation scheme as a disturbance observer to estimate this uncertain disturbance in real-time.

Suppose that $\hat{\tau}_{\rm d} = [\hat{\tau}_{\rm dl}\ \ \hat{\tau}_{\rm dr}]^{\rm T}$ represents the estimated vector of disturbances acting on the left and right wheels, and thus, the estimated error $\tilde{\tau}_{\rm d} = [\tilde{\tau}_{\rm dl}\ \ \tilde{\tau}_{\rm dr}]^{\rm T}$ could be achieved by $\tilde{\tau}_{\rm d} = \hat{\tau}_{\rm d} - \tau_{\rm d}$. The disturbance value and their estimated errors can be governed by $\dot{\tilde{\tau}}_{\rm d} = \dot{\hat{\tau}}_{\rm d}$ due to the slower change rate of the disturbance. Therefore, the controller (12) could be extended to be a new force controller with an additional observer scheme as follows:

$$\begin{aligned}\tau = &\bar{M}\dot{\nu}_{\rm c} + c\bar{M}e_\nu + \bar{V}_{\rm m}\nu_{\rm c} + \hat{\tau}_{\rm d} + \\ &\bar{M}[\sigma_1\tanh(\kappa\Im) + \sigma_2\Im],\end{aligned} \tag{14}$$

$$\dot{\hat{\tau}}_{\rm d} = \mu(\bar{M}^{-1})^{\rm T}\Im. \tag{15}$$

Note that the control law of (15) is essentially an adaptive scheme to observe disturbances for the mobile robot. In this force controller, the parameter $\mu > 0$ determines the convergence time. Generally, bigger of this setting value yields shorter of the convergence time; however, the overshoot of the system variables will increase abruptly. In summary, an improved theory could be given as follows:

Theorem 3 The velocity tracking error $e_\nu = \nu_{\rm c} - \nu$ with uncertain disturbances will asymptotically converge to zero, if the controller (14) and adaptive law (15) is applied to system (4).

Proof An improved positive Lyapunov function is as follows:

$$V_3 = \frac{1}{2}\Im^{\rm T}\Im + \frac{1}{2\mu}\tilde{\tau}_{\rm d}^{\rm T}\tilde{\tau}_{\rm d}.$$

Differentiating V_3 along the trajectory (4) and noting that $\tilde{\tau}_{\rm d}^{\rm T}\dot{\hat{\tau}}_{\rm d} = \dot{\hat{\tau}}_{\rm d}^{\rm T}\tilde{\tau}_{\rm d}$, yields

$$\begin{aligned}\dot{V}_3 = &\Im^{\rm T}(ce_\nu + \dot{\nu}_{\rm c} - \dot{\nu}) + \frac{1}{\mu}\tilde{\tau}_{\rm d}^{\rm T}\dot{\hat{\tau}}_{\rm d} = \\ &\Im^{\rm T}(ce_\nu + \dot{\nu}_{\rm c} + \bar{M}^{-1}\tau + \\ &\bar{M}^{-1}\bar{V}_{\rm m}\nu_{\rm c} + \bar{M}^{-1}\hat{\tau}_{\rm d} - \bar{M}^{-1}\tilde{\tau}_{\rm d}) + \frac{1}{\mu}\tilde{\tau}_{\rm d}^{\rm T}\dot{\hat{\tau}}_{\rm d} = \\ &\Im^{\rm T}[ce_\nu + \dot{\nu}_{\rm c} - \bar{M}^{-1}(\tau - \bar{V}_{\rm m}\nu_{\rm c} - \hat{\tau}_{\rm d})] - \\ &(\Im^{\rm T}\bar{M}^{-1} - \frac{1}{\mu}\dot{\hat{\tau}}_{\rm d}^{\rm T})\tilde{\tau}_{\rm d}.\end{aligned} \tag{16}$$

Substituting (14) and (15) into (16) obtains that:

$$\dot{V}_3 = -\sigma_1\Im^{\rm T}\tanh(\kappa\Im) - \sigma_2\Im^{\rm T}\Im.$$

Obviously, $\dot{V}_3 \leqslant 0$. The Theorem is proved.

5 Simulation study

Simulations are performed with a mobile robot by using the proposed motion and disturbance observer-based adaptive controllers in this section. The simulated physical parameters of a mobile robot are given as follows: $m = 3\,{\rm kg}$, $R = 0.25\,{\rm m}$, $d = 0.1\,{\rm m}$, $r = 0.3\,{\rm m}$. The desired trajectory is supposed to be an eight-shaped curve which is much similar to the practical road, and it could demonstrate the steering and tracking performances of the mobile robot much better. As reported in [6], the eight-shaped trajectory could be defined by

$$x_{\rm r}(t) = \sin t,\ y_{\rm r}(t) = \sin\frac{t}{2},\ t \in [0, T].$$

Meanwhile, the desired orientation angle

$$\theta_{\rm r}(t) = \arctan\frac{\cos(t/2)}{2\cos t},$$

which is generated by the $\dot{y}_{\rm r}$ and $\dot{x}_{\rm r}$ on line. Suppose that the error space of a start point is

$$q_{\rm e}(0) = [x_{\rm e}(0)\ \ y_{\rm e}(0)\ \ \theta_{\rm e}(0)]^{\rm T} = [0.2\ \ -0.2\ \ -\frac{\pi}{2}]^{\rm T}.$$

A full cycle is completed in $T = 2\pi\cdot 2 \approx 14\,{\rm s}$. Note that $q_{\rm e}$ is different from q since $q_{\rm e}$ is the tracking error space introduced by coordinate transformation. In order to satisfy the control performances, the controller's parameters are chosen as follows:

$$\begin{aligned}&\delta = 1,\ k_1 = k_2 = k_3 = 2,\ k_4 = 3,\ \sigma_1 = \sigma_2 = 5,\\ &c_1 = c_2 = 4,\ \kappa = 10,\ \mu = 2000.\end{aligned}$$

Moreover, to assess the performance of the force controller, we also introduce a hypothesis disturbance with step form, representing the worst condition acting on the wheels, to verify the effectiveness of the proposed observer scheme.

Under such hypothesis, Fig.3 demonstrates the practical tracking process of the nonholonomic mobile robot. It indicates that the desired eight shaped trajectory could be tracked well although the initial point start from an arbitrary position. The tracking effects are closely related to the control parameters $k_1,\ k_2,\ k_3,\ k_4$ and δ, which are the main parameters of the motion controller. Furthermore, the orientation angle θ is an interesting variable in eight shaped curve since it yields whether the robot has excellent steering capability. It is expected that $\theta \to \theta_{\rm r}$ as $t \to \infty$ through the motion controller, especially around the center point of the eight shaped curve. The whole tracking process for this orientation parameter is shown in Fig.4, where the dash line yields desired angle trajectory and the solid line is the actual tracking path. The results demonstrate the required tracking and steering performances has been achieved. In order to illustrate the precision of the posture tracking by motion controller, Fig.5 further shows the tracking errors of system states of the mobile robot. This simulation results demonstrate that the tracking error of the robot postures $q_{\rm e} = [x_{\rm e}\ y_{\rm e}\ \theta_{\rm e}]^{\rm T}$ are globally stabilized and rapidly converged to zero in 5 s.

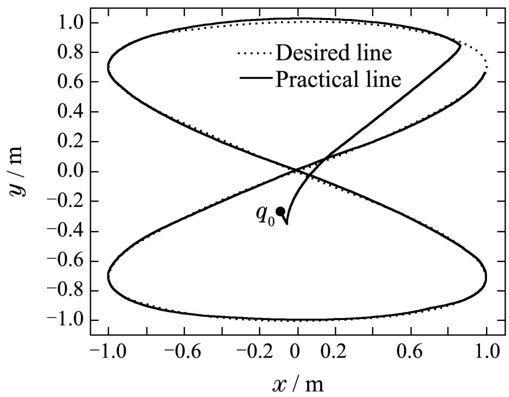

Fig. 3 Tracking for an eight-shaped trajectory

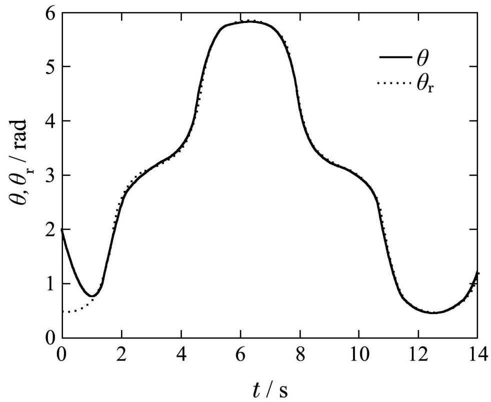

Fig. 4 Tracking process of orientation angle

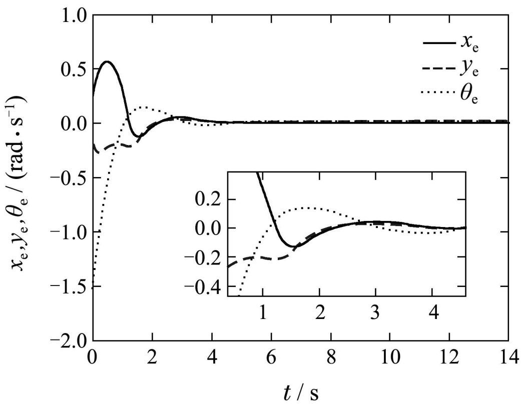

Fig. 5 Posture errors of the mobile robot

Figure 6 tells the estimation process for the uncertain disturbance with the system's observer scheme. Here, abrupt frictions, which yield an extremely worst condition, are supposed to be acted on the wheels to verify the disturbances adaptivity characteristic of the observer-based scheme. The disturbance $\tau_{\rm dl}$ acting on the left wheel occurs between 20 kN and 40 kN at 5 s and 10 s, while the disturbance $\tau_{\rm dr}$ acting on the right one occurs between 25 kN and 55 kN at 2.5 s and 7.5 s. With the chosen control parameter $\mu = 2000$, the observation values are agrees well with the required estimation performances. Generally, by increasing the controller's parameter μ, the observe accuracy and convergence time are improved, while the observe overshoots are abruptly increasing. Additionally, the control parameter κ is also an important control coefficient of the hyperbolic tangent function that could determine the degree of continuity of the control signals. The simulation also confirms the chosen constant $\kappa = 10$ is acceptable in this case.

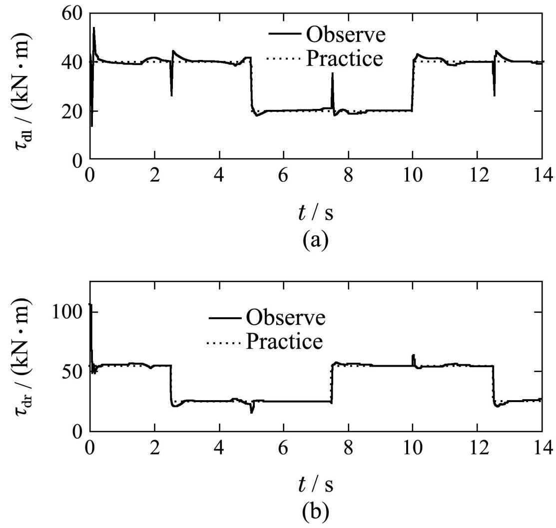

Fig. 6 Response of the observation process for the disturbances

6 Conclusion

Path following control problem of a nonholonomic mobile robot was investigated in this study. To deal with the nonholonomic constraint affected on the system's kinematic model which is related to robot's postures, the backstepping technique based on a new function $x/(1+x^2)$ is applied to construct an additional state variable $\bar{x}_e$. With the derived motion controller, a more tracking precision of robot's postures was achieved. Additionally, a force controller made up of an integral sliding mode control method and a disturbance observer, was also developed to resolve the uncertain problem of terrain friction acting on the wheels. This adaptive robust control law could regulate the controller according to the dynamic exploration environment in real-time. Such motion/force multi-objective could be realized harmoniously by the proposed double closed-loop control structure. By introducing the virtual velocity, a motion/force sensitive target for mobile robot could be coordinately controlled simultaneously. Further work will develop experiments to verify the effectiveness of the proposed control methods.

References:

[1] SAMSON C. Control of chained systems application to path-following and time-varying point-stabilization of mobile robots [J]. *IEEE Transactions on Automatic Control*, 1995, 40(1): 64 – 77.

[2] YUE M, HU P, SUN W. Path following of a class of non-holonomic mobile robot with underactuated vehicle body [J]. *IET Control Theory and Applications*, 2010, 4(10): 1898 – 1904.

[3] LI Z, ZHANG Y. Robust adaptive motion/force control for wheeled inverted pendulums [J]. *Automatica*, 2010, 46(8): 1346 – 1353.

[4] DIXON W, JIANG Z, DAWSON D. Global exponential setpoint control of wheeled mobile robots: a Lyapunov approach [J]. *Automatica*, 2000, 36(11): 1741 – 1746.

[5] SANKARANARAYANAN V, MAHINDRAKAR A. Control of a class of underactuated mechanical systems using sliding modes [J]. *IEEE Transaction on Robotics*, 2009, 25(2): 459 – 467.

[6] ORIOLO G, LUCA A, VENDITTELLI M. WMR control via dynamic feedback linearization: Design, implementation, and experimental validation [J]. *IEEE Transactions on Control Systems Technology*, 2002, 10(6): 835 – 852.

[7] JIANG Z, LEFEBER E, NIJMEIJER H. Saturated stabilization and tracking of a nonholonomic mobile robot [J]. *Systems and Control Letters*, 2001, 42(5): 327 – 332.

[8] PARK B, YOO S, PARK J, et al. A simple adaptive control approach for trajectory tracking of electrically driven nonholonomic mobile robots [J]. *IEEE Transactions on Control Systems Technology*, 2010, 18(5): 1199 – 1206.

[9] HOU Z, ZOU A, CHENG L, et al. Adaptive control of an electrically driven nonholonomic mobile robot via backstepping and fuzzy approach [J]. *IEEE Transactions on Control Systems Technology*, 2009, 17(4): 803 – 815.

[10] LI Z, ZHANG J, YANG Y. Motion control of mobile under-actuated manipulators by implicit function using support vector machines [J]. *IET Control Theory and Applications*, 2010, 4(11): 2356 – 2368.

[11] LI Z, GE S, ADAMS M, et al. Adaptive robust output-feedback motion/force control of electrically driven nonholonomic mobile manipulators [J]. *IEEE Transactions on Control Systems Technology*, 2008, 16(6): 1308 – 1315.

[12] HASHEMI E, JADIDI M, JADIDI N. Model-based PI-fuzzy control of four-wheeled omni-directional mobile robots [J]. *Robotics and Autonomous Systems*, 2011, 59(11): 930 – 942.

[13] YUE M, SUN W, HU P. Sliding mode robust control for two-wheeled mobile robot with lower center of gravity [J]. *International Journal of Innovative Computing, Information and Control*, 2011, 7(2): 637 – 646.

[14] JIANG Z, NIJMEIJER H. A recursive technique for tracking control of nonholonomic systems in chained form [J]. *IEEE Transactions on Automatic Control*, 1999, 44(2): 265 – 279.

[15] CHIU C, PENG Y, LIN Y. Robust intelligent backstepping tracking control for wheeled inverted pendulum [J]. *Soft Computing*, 1999, 15(10): 2029 – 2040.

[16] DONG W. Flocking of multiple mobile robots based on backstepping [J]. *IEEE Transactions on Systems Man and Cyvernetics, Part B: Cybernetics*, 2011, 41(2): 414 – 424.

[17] HU Q, MA G. Variable structure control and active vibration suppression of flexible spacecraft during attitude maneuver [J]. *Aerospace Science and Technology*, 2005, 9(4): 307 – 317.

[18] HU Q, MA G, XIE L. Robust and adaptive variable structure output feedback control of uncertain systems with input nonlinearity [J]. *Automatica*, 2008, 44(2): 552 – 559.

[19] SONG G, GU H. Active vibration suppression of a smart flexible beam using a sliding mode based controller [J]. *Journal of Vibration and Control*, 2007, 13(8): 1095 – 1107.

[20] KANAYAMA Y, KIMURA Y, MIYAZAKI F, et al. A stable tracking control method for an autonomous mobile robot [C] //*IEEE International Conference on Robotics and Automation*. Cincinnati, USA: IEEE, 1990: 384 – 389.

[21] HU Q, ZHANG Y, HUO X, et al. Adaptive integral-type sliding mode control for spacecraft attitude maneuvering under actuator stuck failures [J]. *Chinese Journal of Aeronautics*, 2011, 24(1): 32 – 45.

作者简介:

岳 明 (1975–), 男, 博士, 副教授, 目前研究方向为机电系统动力学与控制、非线性控制理论与应用, E-mail: yueming@dlut.edu.cn;

王 爽 (1979–), 女, 博士, 在做博士后研究工作, 目前研究方向为车辆动态系统仿真与控制, E-mail: wangshuang0702@126.com;

张永顺 (1965–), 男, 博士, 教授, 目前研究方向为机器人技术与应用.